

# Modeling VLF propagation in the Earth-ionosphere waveguide using the discontinuous Galerkin method.

*Forrest Foust*<sup>1</sup>, *Timothy Bell*<sup>2</sup>, and *Umrhan Inan*<sup>3</sup>

<sup>1</sup>Stanford University Electrical Engineering Department, 350 Serra Mall, David Packard Building,  
Stanford University, CA, USA, ffoust@stanford.edu

<sup>2</sup>tbell@stanford.edu

<sup>3</sup>inan@stanford.edu

## Abstract

Modeling of scattering of very low frequency (VLF, 3-30 kHz) waves from ionospheric disturbances remains a significant computational challenge due to the strong inhomogeneity and anisotropy naturally present at these frequencies. The discontinuous Galerkin (DG) method on unstructured grids can lead to very efficient formulations in strongly inhomogeneous materials. We discuss a generic method to incorporate any linear, frequency-dependent permittivity or permeability in the nodal DG framework (including PMLs, ferrites, and cold plasmas) and apply the resulting scheme to modeling the VLF scattered field from a density perturbation in the lower ionosphere.

## 1 Introduction

Modeling very low frequency (VLF, 3-30 kHz) wave propagation in the Earth-ionosphere waveguide remains an important and computationally difficult problem. In free space, VLF waves have typical wavelengths in the range of tens of km. However, the situation rapidly changes in the partially ionized upper atmosphere. Near the VLF reflection height for a typical mid-latitude ionosphere at 24 kHz (approximately 85 km at night), the wavelength can drop to less than a quarter of its free-space value for propagation parallel to the background magnetic field, or even zero for non-parallel propagation. There have been many approaches to modeling propagation and scattering of VLF waves in the Earth-ionosphere waveguide. Full-wave models such as that used in the Long Wave Propagation Capability (LWPC) [6] solve a series of full-wave solutions within spatially-uniform “slabs” combined with mode-coupling calculations to propagate the fields to adjacent slabs. This approach assumes that the inhomogeneities have no variation transverse to the direction of propagation. Another approach to handle the inhomogeneity along a propagation path has been discussed in [4], which uses the Born approximation to model the inhomogeneity as a set of equivalent currents. This approach is powerful but is limited to relatively mild density perturbations. Recently, generic field solvers like FDTD have gained in popularity and have been successfully applied to VLF propagation and scattering off ionospheric disturbances [5, 7, 2]. These simulations are typically bound by the number of unknowns required to accurately discretize the space. Typical rule-of-thumb guidelines state that on the order of 5 to 10 cells per wavelength are required to accurately represent a solution using FDTD. While this is not necessarily prohibitive for moderately-sized problems (on the order of a few hundred km per spatial dimension) *within* the Earth-ionosphere waveguide, the situation rapidly degrades above the VLF reflection height, where the wavelength can easily drop to less than a quarter of its free-space value. For reasonable accuracy on a fixed FDTD grid, then, the grid spacing must be chosen based on the *smallest* wavelength expected to be present in the solution, and thus is enormously prohibitive for a fixed grid. While FDTD has been used on semi-structured and fully-unstructured grids, doing so reduces the formal order of accuracy of the scheme from second to first order.

In this paper, we discuss the application of a relatively new class of techniques known as *discontinuous Galerkin* (DG) methods to the problem of wave propagation in the Earth-ionosphere waveguide. Since it is straightforward to use the DG method on unstructured grids and doing so has no impact on the formal order of accuracy, we can manage the scale problem by sampling more finely only where it is needed, i.e., near the VLF reflection height, while using a coarser grid elsewhere. This approach allows accurate and flexible simulation of scattering off ionospheric disturbances in the VLF regime with fewer restrictions on the types

or magnitudes of the plasma density perturbations that can be modeled.

## 2 Nodal discontinuous Galerkin formulation

The discontinuous Galerkin (DG) formulation approximates the solution on a domain by first approximating the solution *local* to a single finite element using a basis (typically polynomial) and then connecting that solution to neighboring elements using a numerical flux function. The solution method is effectively a hybrid between finite volume and finite element techniques. The nodal DG method begins by approximating a solution  $\mathbf{u}^e(\mathbf{x})$  on an element  $e$  with an interpolating Lagrange polynomial basis  $\phi_i(x)$  as:

$$\mathbf{u}^e(\mathbf{x}) \approx \sum_{i=1}^N \mathbf{u}(\mathbf{x}_i) \phi_i^e(\mathbf{x}) \quad (1)$$

Substituting this into the generic conservation law  $\frac{\partial \mathbf{u}}{\partial t} + \nabla \cdot F(\mathbf{u}) = 0$ , where  $F$  is a tensor, that is:

$$\nabla \cdot F(\mathbf{u}) = \frac{\partial}{\partial x} F_x(\mathbf{u}) + \frac{\partial}{\partial y} F_y(\mathbf{u}) + \frac{\partial}{\partial z} F_z(\mathbf{u}) \quad (2)$$

Then substituting and integrating by parts twice, we have the strong form of the DG scheme:

$$\int_V \left( \frac{\partial \mathbf{u}^e}{\partial t} + \nabla \cdot F^e(\mathbf{x}) \right) \phi_i^e(\mathbf{x}) d\mathbf{x} = \oint_S \hat{\mathbf{n}} \cdot (F^e - F^*) \phi_i^e(\mathbf{x}) d\mathbf{S} \quad (3)$$

The function  $F^*$  denotes a numerical flux. For the scheme to be well-posed,  $F^*$  must typically be chosen in such a way that it combines the fluxes interior to an element ( $F^-$ ) and exterior to an element ( $F^+$ ) in a physically self-consistent way. For Maxwell's equations, we have [3], where we have dropped the superscript  $e$  for clarity, understanding that this is the solution defined only on a single element  $e$ :

$$M \frac{\partial(\epsilon \mathbf{E})}{\partial t} + S F_E + M \mathbf{J} = \oint_S \hat{\mathbf{n}} \cdot (F_E - F_E^*) \phi_i(\mathbf{x}) d\mathbf{S} \quad (4)$$

$$M \frac{\partial(\mu \mathbf{H})}{\partial t} + S F_H + M \mathbf{J}_m = \oint_S \hat{\mathbf{n}} \cdot (F_H - F_H^*) \phi_i(\mathbf{x}) d\mathbf{S} \quad (5)$$

The matrices  $M$  and  $S$  are the standard mass and stiffness matrices, respectively:

$$M_{ij} = \int \phi_i(\mathbf{x}) \phi_j(\mathbf{x}) d\mathbf{x} \quad S_{ij} = \int \phi_i(\mathbf{x}) \frac{d\phi_j}{d\mathbf{x}} d\mathbf{x}, \quad (6)$$

and the fluxes along the normal are:

$$\hat{\mathbf{n}} \cdot F_E = -\hat{\mathbf{n}} \times \mathbf{H} \quad \hat{\mathbf{n}} \cdot F_H = \hat{\mathbf{n}} \times \mathbf{E} \quad (7)$$

We use a standard flux as described in [3]:

$$\hat{\mathbf{n}} \cdot (F_E - F_E^*) = \frac{1}{(Z^+ + Z^-)} (\alpha \hat{\mathbf{n}} (\hat{\mathbf{n}} \cdot [\mathbf{E}]) - \alpha [\mathbf{E}] - Z^+ \hat{\mathbf{n}} \times [\mathbf{H}]) \quad (8)$$

$$\hat{\mathbf{n}} \cdot (F_H - F_H^*) = \frac{1}{(Y^+ + Y^-)} (\alpha \hat{\mathbf{n}} (\hat{\mathbf{n}} \cdot [\mathbf{H}]) - \alpha [\mathbf{H}] + Y^+ \hat{\mathbf{n}} \times [\mathbf{E}]), \quad (9)$$

where the + and - superscripts denote the field values exterior and interior to the current element, and  $[u] = u^- - u^+$  is the field difference at the face.

### 3 Anisotropic and Dispersive Materials

One key distinguishing feature of the nodal DG method is that the solution is solved at *interpolation* points, that is, the nodal values *are* the solution at those points. Thus, the relationship between a current  $\mathbf{J}(\mathbf{x}_i)$  and the field  $\mathbf{E}(\mathbf{x}_i)$  at a point  $\mathbf{x}_i$  is direct; no spatial averaging to colocate the fields is required. We begin by noting that any anisotropic permittivity can be represented by an equivalent conductivity tensor via the relation  $\epsilon(\omega) = \epsilon_0(\epsilon_{\infty,r} - \sigma(\omega)/(j\omega\epsilon_0))$ , where we have used the Fourier transform convention  $\partial/\partial t \rightarrow -j\omega$ . The relative permittivity at infinity  $\lim_{\omega \rightarrow \infty} \epsilon_r(\omega) = \epsilon_{\infty,r}$  is simply equal to the unit dyad  $I$  for a physical medium, but it is often useful in a computational setting to choose different values. We also note that in a plasma, the conductivities for each species sum, that is,  $\mathbf{J}_{\text{plasma}}(\omega) = \sigma_e(\omega)\mathbf{E}(\omega) + \sigma_i(\omega)\mathbf{E}(\omega) + \dots$ . We wish to rewrite the frequency-dependent relationship  $\mathbf{J}(\omega) = \sigma(\omega)\mathbf{E}(\omega)$  as a first-order ODE:

$$\begin{aligned} x' &= Ax + B\mathbf{E} \\ \mathbf{J} &= Cx + D\mathbf{E} \end{aligned} \quad (10)$$

We begin by writing the plasma conductivity as a matrix of ratios of polynomials, where we are denoting the complex frequency  $-j\omega$  as  $s$ :

$$\sigma(s) = \frac{\epsilon_0 \omega_p^2}{d(s)} \begin{bmatrix} s^2 + 2\nu s + \nu^2 + \omega_{cx}^2 & \omega_{cz}s + \omega_{cx}\omega_{cy} + \nu\omega_{cz} & -\omega_{cy}s - \nu\omega_{cy} + \omega_{cx}\omega_{cz} \\ -\omega_{cz}s + \omega_{cx}\omega_{cy} - \nu\omega_{cz} & s^2 + 2\nu s + \nu^2 + \omega_{cy}^2 & \omega_{cx}s + \nu\omega_{cx} + \omega_{cy}\omega_{cz} \\ \omega_{cy}s + \nu\omega_{cy} + \omega_{cx}\omega_{cz} & -\omega_{cx}s - \nu\omega_{cx} + \omega_{cy}\omega_{cz} & s^2 + 2\nu s + \nu^2 + \omega_{cz}^2 \end{bmatrix} \quad (11)$$

where  $d(s) = (s + \nu)(s^2 + 2s\nu + \nu^2 + |\omega_c|^2)$  and  $\omega_c$  denotes the *signed gyrofrequency vector*, that is,  $\omega_c = (q\mathbf{B}_0)/m$ . We then use an SVD-based balanced minimal realization algorithm to convert this tensor into a first-order system [1]. The procedure requires finding the SVD of the Hankel matrix formed from the Markov parameters computed by expanding  $\sigma(s)$  in a series as  $\sigma(s) = \sigma_0 + \sigma_1 s^{-1} + \sigma_2 s^{-2} + \dots$ . A minimal realization will ensure that the state vector  $x$  is as small as possible; we recognize that other realizations are also possible and may have more desirable properties like sparsity in the state transition and mixing matrices, but we find that this algorithm is robust for a wide variety of plasma parameters. We do note, however, that it is necessary to pre-scale the frequencies, otherwise the zero singular values (to within roundoff) will not be clearly delineated from the non-zero singular values. This is done by scaling  $s$  such that  $\hat{s} = s/k$ , where  $k$  is chosen heuristically such that the roots of the characteristic polynomial are approximately less than 1. After the realization procedure yields the scaled matrices  $\hat{A}$ ,  $\hat{B}$ ,  $\hat{C}$ , and  $\hat{D}$ , the actual matrices can be found by unscaling as:  $A = k\hat{A}$ ,  $B = k\hat{B}$ ,  $C = \hat{C}$ , and  $D = \hat{D}$ .

We note that precisely the same procedure can be used for any anisotropic, dispersive material, including ferrites and the tensor form of the PML (i.e. the UPML). An anisotropic material itself can be terminated by an anisotropic PML as described in [8] and then realized via exactly the same procedure.

### 4 Numerical tests

To demonstrate the validity of the cold plasma formulation, we show that the scheme reproduces theoretical cold plasma modes. We discretize a 1D space 40 km in size with 800 grid cells and use a 2nd order polynomial basis. The electron density is set to  $4 \cdot 10^9 \text{ m}^{-3}$  and background magnetic field  $B_0 = 21682.4 \cdot 10^{-9} \text{ T}$ . We “ping” the system with a differentiated Gaussian, well-localized both in time and space, and record the resulting fields as a function of space and time. A 2D Fourier transform followed by normalization then yields an experimental  $\omega - k$  diagram. We repeat the procedure for both parallel and perpendicular propagation. Both are in excellent agreement with theory, as shown in Figure 1.

The PML is implemented using the complex frequency-shifted tensor PML. The PML boundary is ungraded, yet performs very well, demonstrating DG’s superior handling of discontinuities. We place a dipole source at the center of the space and truncate with a PML. The resulting electric fields are shown in Figure 2(a).

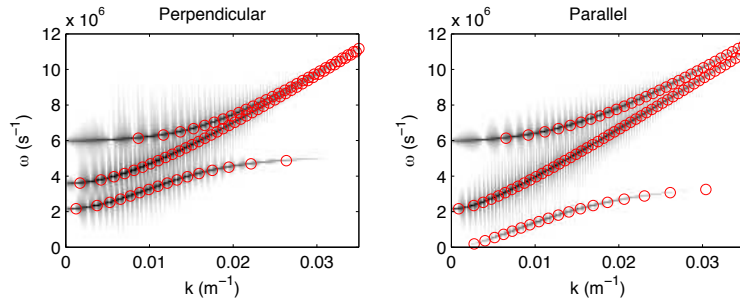


Figure 1: Simulated and theoretical cold plasma dispersion relations. The red dots show the location in  $\omega - k$  space of the cold plasma modes for perpendicular (left) and parallel (right) propagation, superimposed on the 2D FFT of the fields resulting from pinging a cold plasma in simulation.

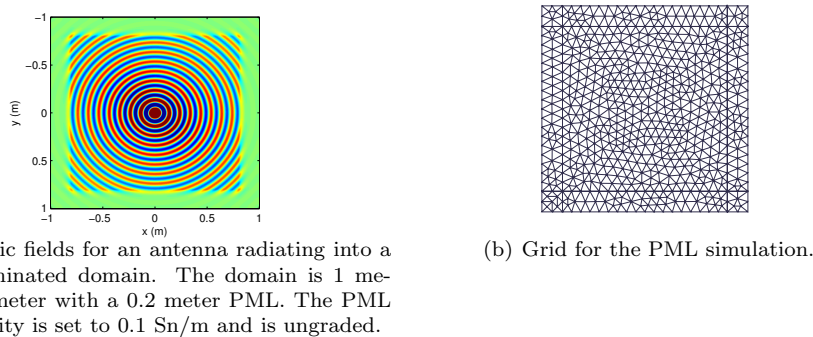


Figure 2: DG-FEM simulation of a domain truncated by a PML.

## References

- [1] Panos J. Antsaklis. *Linear systems* / Panos J. Antsaklis, Anthony N. Michel. McGraw-Hill, New York, 1997.
- [2] S. A. Cummer. Modeling electromagnetic propagation in the Earth-ionosphere waveguide. *IEEE Transactions on Antennas and Propagation*, 48:1420–1429, September 2000.
- [3] Jan S. Hesthaven and Tim Warburton. *Nodal Discontinuous Galerkin Methods: Algorithms, Analysis, and Applications*. Springer Publishing Company, Incorporated, 1st edition, 2007.
- [4] N. G. Lehtinen, R. A. Marshall, and U. S. Inan. Full-wave modeling of early VLF perturbations caused by lightning electromagnetic pulses. *Journal of Geophysical Research (Space Physics)*, 115(A14):0–+, July 2010.
- [5] R. A. Marshall, U. S. Inan, and T. W. Chevalier. Early VLF perturbations caused by lightning EMP-driven dissociative attachment. *Geophysical Research Letters*, 35:21807–+, November 2008.
- [6] R. A. Pappert and J. A. Ferguson. VLF/LF mode conversion model calculations for air to air transmissions in the earth-ionosphere waveguide. *Radio Science*, 21:551–558, August 1986.
- [7] W. B. Peter, M. W. Chevalier, and U. S. Inan. Perturbations of midlatitude subionospheric VLF signals associated with lower ionospheric disturbances during major geomagnetic storms. *Journal of Geophysical Research (Space Physics)*, 111(A10):3301–+, March 2006.
- [8] F.L. Teixeira and W.C. Chew. General closed-form pml constitutive tensors to match arbitrary bianisotropic and dispersive linear media. *Microwave and Guided Wave Letters, IEEE*, 8(6):223–225, June 1998.